Numerical modelling of earthquake strong ground motion in the area of Vittorio Veneto (NE Italy)

G. Laurenzano and E. Priolo

Istituto Nazionale di Oceanografia e di Geofisica Sperimentale, Udine, Italy

(Received: Noveber 17, 2005; accepted: January 16, 2008)

ABSTRACT In this study, we compute some ground motion scenarios for the area surrounding the town of Vittorio Veneto (NE Italy). We use two different numerical approaches. In the first approach, called EXWIM, the earthquake source is represented by a rupture which propagates along an extended fault with a prescribed kinematics. With this method, we build ground motion scenarios at a regional scale for the Vittorio Veneto area. We consider two reference earthquakes, i.e. the historical M=5.8, Cansiglio event of October 18, 1936 and a hypothetical M=6.7 earthquake occurring in the Montello area, directly SW of Vittorio Veneto. With the second approach, called SPEM 2D, we take into account the effects of a complex crustal structure and local soil conditions on the propagating seismic waves. This method is used for the construction of a detailed ground shaking scenario for the Vittorio Veneto area and to estimate the effect of the wave-field propagation on the ground motion through the complex Alpago-Cansiglio geological structure.

1. Introduction

This work has been developed through the three-year research project entitled 'Scenarios of seismic damages in Friuli and Veneto' funded by the National Group for the Defence against Earthquakes (GNDT). Although the goal of the overall project was to provide an estimate of the seismic risk in the Veneto-Friuli area (NE Italy), most studies have focused on the town of Vittorio Veneto, in virtue of its historical and artistic importance as well as for its geographical location and economic importance.

We have built some strong ground motion scenarios in the area of Vittorio Veneto by using deterministic numerical approaches where the contributions of source processes, propagation-path characteristics and site effects are taken into account. Two different numerical methods have been used. The first method, called EXWIM, considers the effects on the seismic wave-field of the spatial extension of the seismic source, modelled as a rupture propagating along a plane fault. The second method, called SPEM 2D, accounts for the effects of a complex crustal structure and local soil conditions (topography included) on the propagating seismic wavefield, although it defines the source in a simplified way.

In this paper, we first describe the application of EXWIM in the construction of complete ground motion scenarios at regional scale for two reference earthquakes, i.e. the historical Cansiglio earthquake of October 18, 1936, with estimated magnitude M=5.8, and a hypothetical M=6.7 earthquake associated to a supposed seismogenic structure located beneath the nearby Montello area. Then, a detailed scenario at Vittorio Veneto is constructed by the SPEM 2D

method, considering a complex structural model and local site conditions. In this case, the reference earthquake is the historical *M*=5.8 Cansiglio event.

2. Scenarios for the *M*=5.8 Cansiglio earthquake at regional scale

The study is divided into three parts. In the first part, the ground motion is estimated for a point source located at different hypocentral depths and for different crustal models. In this way, we estimate the sensitivity of the results with respect to different assumptions, and constrain the overall prediction. A validation of the methodology, by modelling some recent, small events that occurred in the same area and have been recorded by the seismometric stations of the OGS network, has been performed. Finally, the rupture propagation along an extended fault is considered. These simulations point out the importance of the effects of both source finiteness and rupture propagation along the fault on the ground motion predictions.

2.1. Study area and structural model

The study area (Fig. 1) is a square with a 50 km side centred at the epicentre of the reference earthquake. It is sampled by 441 receivers, with 2.5 km of inter-spacing.

The *M*=5.8 event, that occurred on October 18, 1936 has been associated to a thrust in the Alpago-Cansiglio area. The source parameters were provided by the project task devoted to the characterization of the seismogenic sources at the end of the first year of the project, and were obtained by a preliminary inversion of the macroseismic intensity distribution (CFT catalogue; Boschi *et al*., 1997) using the KF function (Pettenati and Sirovich, 2003). The focal mechanism is oblique, with a strong reverse fault character (ϕ = 212°, δ = 52°, λ = 41°). The depth ranges from 8 to 13 km. The seismic moment associated to this event is $M_0 = 3.7 \times 10^{17}$ N·m (Hanks and Kanamori, 1979; Marcellini, 1995).

Two different sets of 1D models, representing the crustal structure of the study area, were prepared independently from each other. Having different and independent models is very important, as it allows us to estimate the sensitivity of the results with respect to different starting assumptions, and to better constrain the overall prediction. The 1D models are characterized by two levels of approximation.

The first set consists of two structural models corresponding to the average geological structure of north-eastern Italy. For the second set, we assume that the area is divided into different compartments corresponding to different structural elements and associate a specific structural model at each compartment. The compartments (Fig. 2) are the plane area (p), the foot-hill zone (pd), the Alpine valley (m2) and the mountainous in area (m1), respectively. The level of detail has been further improved by adding a surface layer for each specific compartment that takes into account the uppermost coverage (Quaternary deposits) and the topographic elevation in a simplified way.

2.2. Point source simulations and validation of the methodology

In a first part of the study, we performed a number of simulations using a point source model with the aim of evaluating different starting assumptions, such as different source depths and structural models. Obviously, with this kind of simulation, some important aspects of the ground

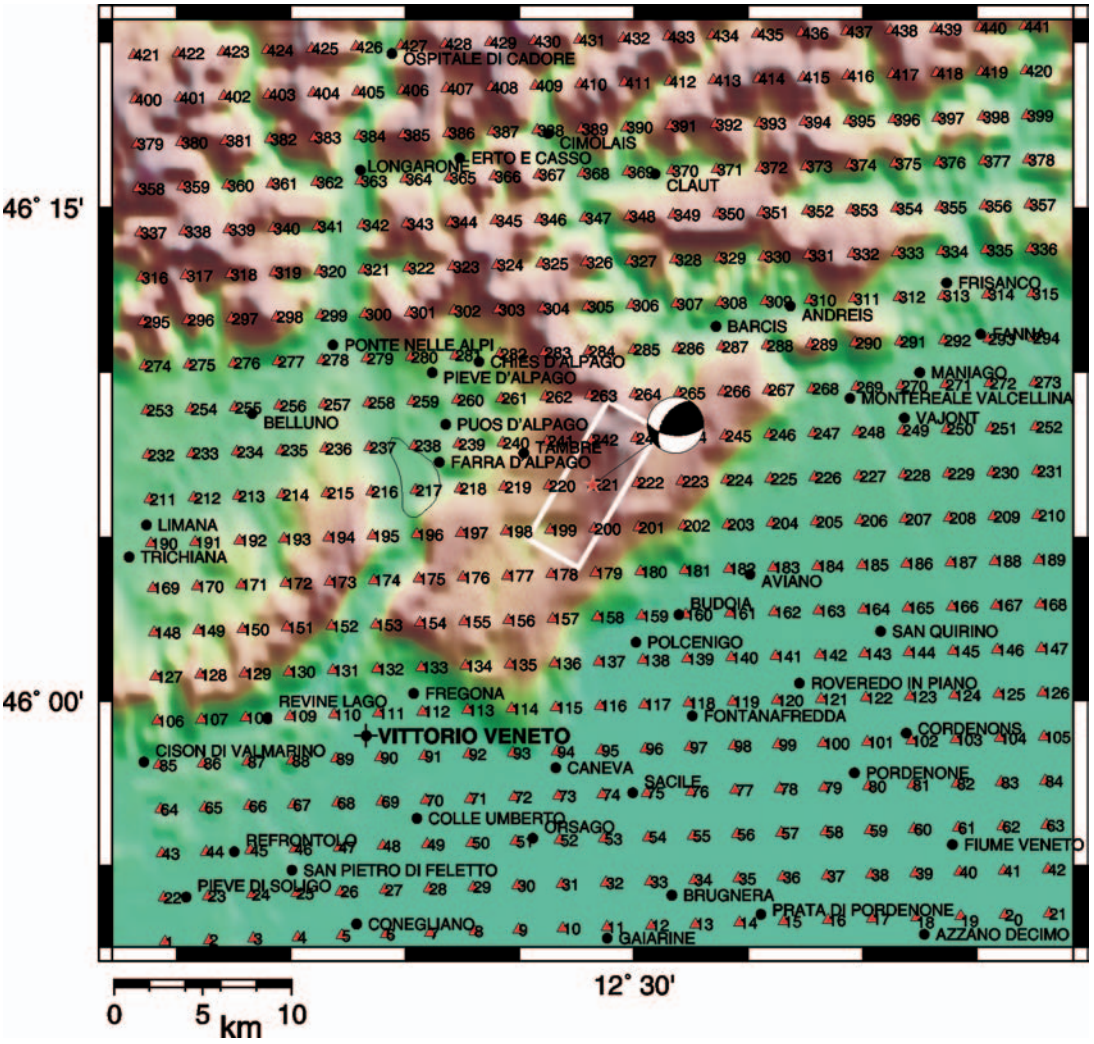

Fig. 1 - Map showing the study area, the receiver location and the fault geometry for the *M*=5.8, Cansiglio earthquake scenarios.

motion induced by earthquakes are neglected, such as the effect due to the source finiteness (rupture propagation, directivity effects, ...). For this reason, the results of the point source simulations mainly reflect the source radiation pattern and have the principal purpose of estimating the relative differences due to different input parameters. The modelling is performed using the Wavenumber Integration Method [WIM: Herrmann and Wang (1985), Herrmann (1996a, 1996b)], which solves the 3D full wave equation in a horizontally layered medium. The synthetic seismograms contain all the phases and are accurate in both the near and far field. The maximum frequency of the modelled waveforms is set at 4.5 Hz.

Firstly, the effect due to source depth variation has been analyzed. Source depths of z = 8, 10, 12, 15, 18 km have been simulated; these cover the whole range of hypocentral depths proposed

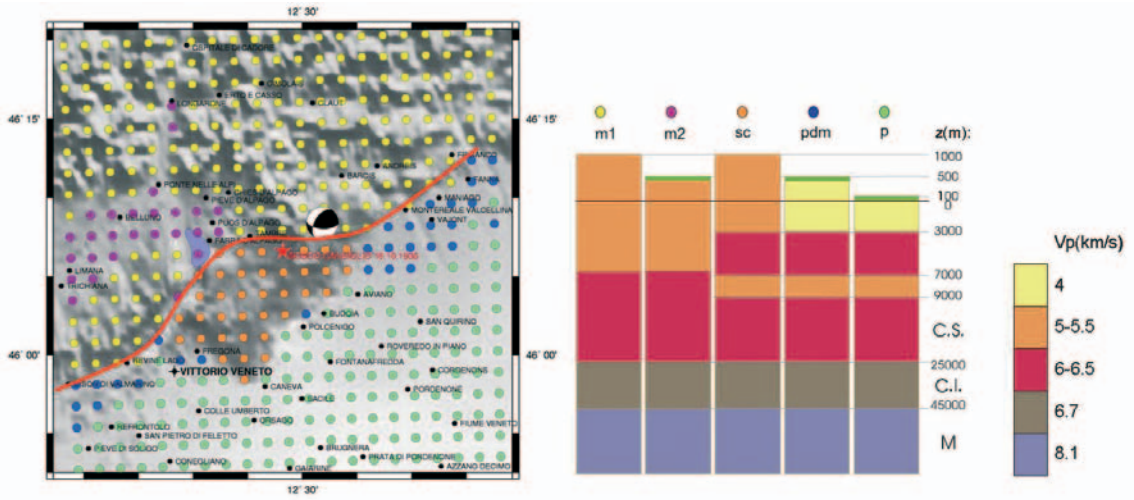

Fig. 2 - P-velocity model used in the simulations (Poli and Zanferrari, personal communication) and the map of the areas corresponding to different structures.

by different authors. The peak ground acceleration (*PGA*) maps obtained (Fig. 3) display two asymmetric lobes of maximum ground shaking, one being located NW of the epicentre by the Alpago-Cansiglio highlands, and the other, SE, around the villages of Budoia and Polcenigo. These lobes directly represent the contribution of the source radiation pattern. For increasing depths, the distance between the two lobes increases and the amplitudes decrease.

Then, the effect of the structural model variation was analysed. The comparison of the results obtained, on the one hand for different crustal structures, and on the other, for models with a specific surface layer for each compartment (Fig. 3) shows that the ground motion is influenced more by the presence of surface, low-velocity layers than by strong, crustal structure variations.

The numerical approach was validated by simulating some weak, local events that were recently recorded by the OGS seismometric network (Fig. 4, left panel). Fig. 4, right panel, compares the seismograms and amplitude spectra predicted and recorded at two stations during the M=3.2 Ponte nelle Alpi earthquake of May 6, 2000. A reverse fault mechanism has been assumed. The agreement is pretty good, and in particular, both arrival times and amplitudes of the main phases are correctly reproduced.

2.3. Extended source simulations

We take into account the effects of source finiteness, i.e. slip distribution, hypocenter location and kinematics of the rupture propagation, using an extended source. The source of the M=5.8 event has been modelled with a rectangular surface 9 km long and 5.4 km wide (Wells and Coppersmith, 1994), NW dipping and extending into a depth of 10 to 14 km (Fig. 1). The structural model assumed in this simulation is displayed in Fig. 2. This model is characterized by different crustal structures and takes into account the local conditions at each site, in a simplified way.

Unlike the simulations performed for the point source approximation, in this case, we decided

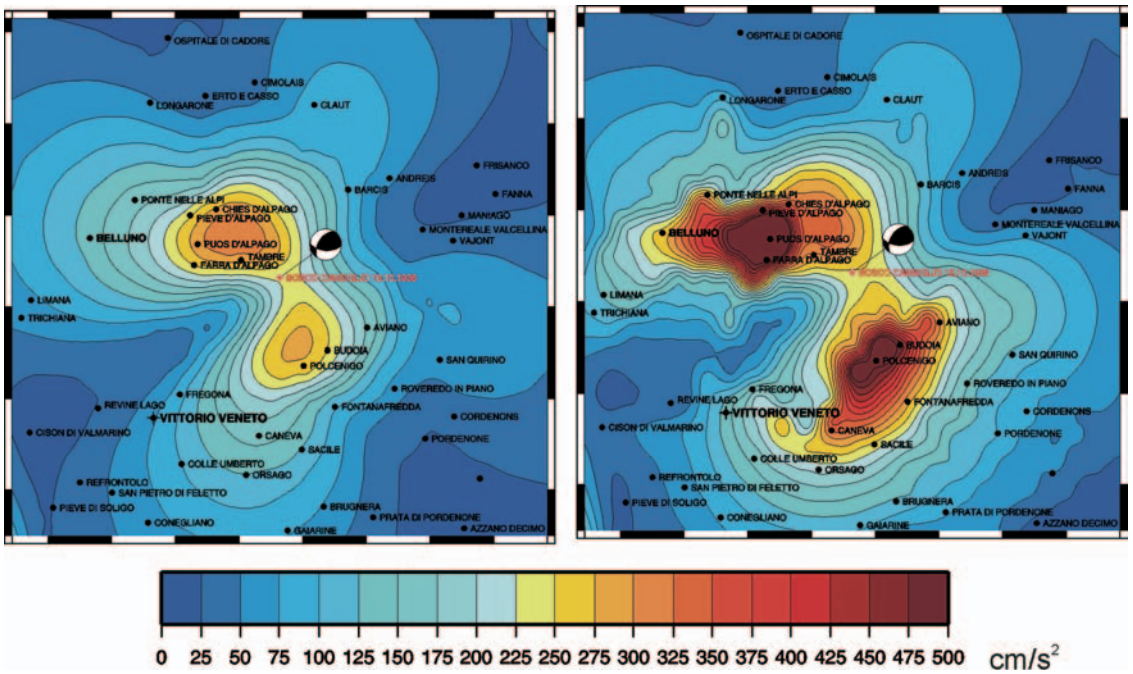

Fig. 3 - *PGA* values obtained using different models: with rock (left) and with soil specified (right) at surface. The hypocentral depth is 12 km.

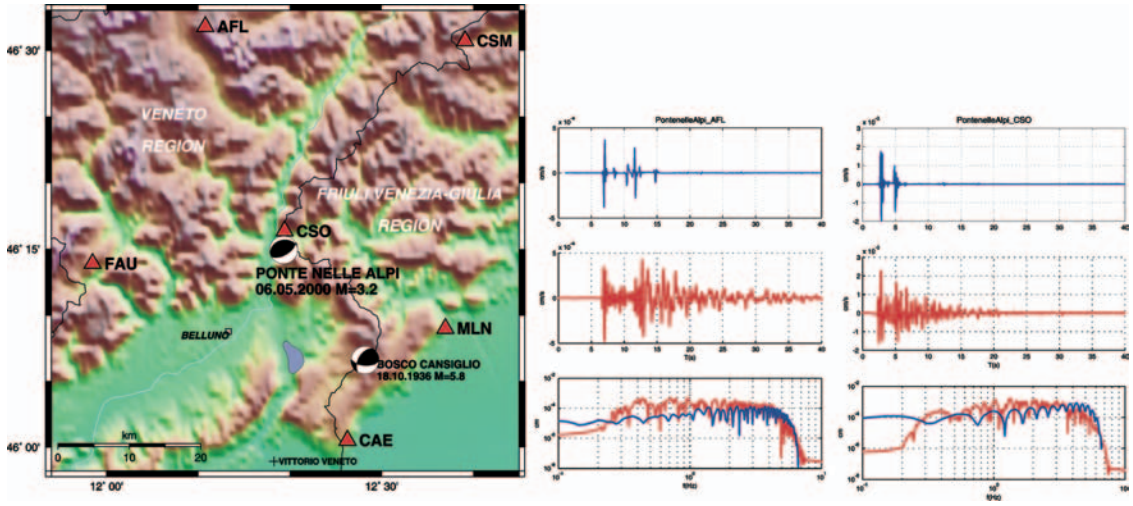

Fig. 4 - Left panel: epicenter location of the *M*=3.2, Ponte nelle Alpi event and the location of the seismometric stations, used for the validation. Right panel: synthetic seismograms and amplitude spectra (vertical component) computed (in blue) and recorded (in red) at two stations.

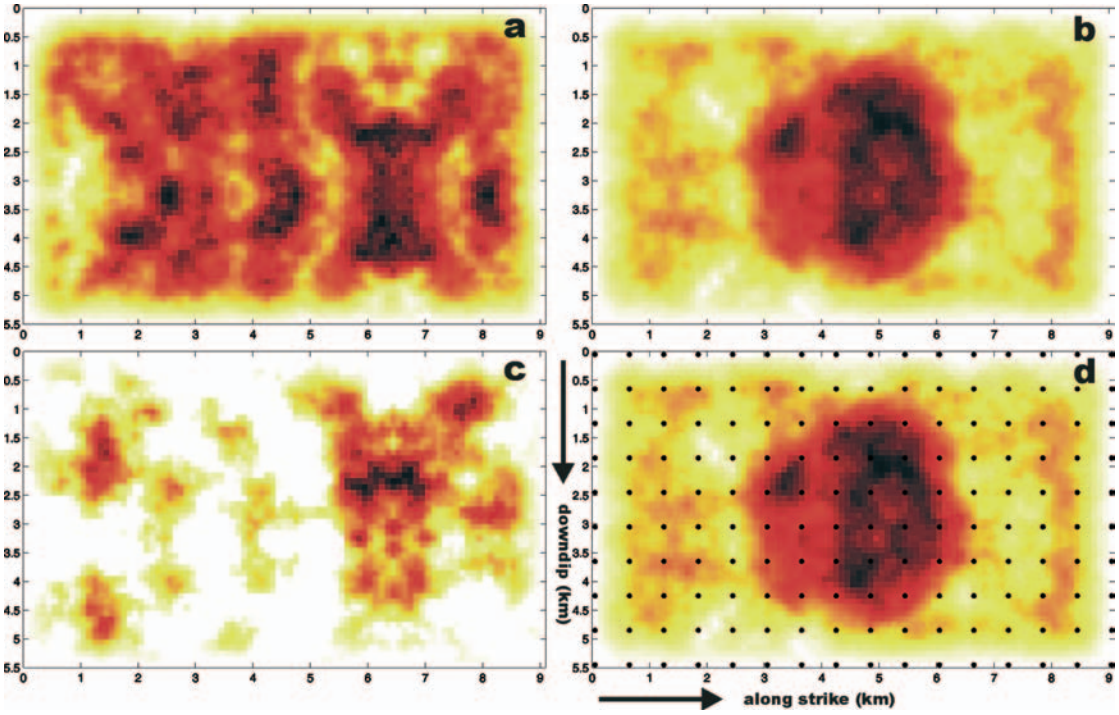

Fig. 5 - Seismic moment distribution characterized by: a) seismic moment spread irregularly along the whole fault; b) large central asperity; c) several small asperities. The black dots in panel d) indicate the nucleation point locations.

to extend the high-frequency band in order to correctly reproduce the near-fault effects. For this reason, we adopted a hybrid stochastic-deterministic approach where composite broadband seismograms, that span the entire frequency range of interest, are obtained as a sum of deterministic low-frequency complete seismograms and a stochastic high-frequency contribution. Our computational procedure consists in the following: 1) discretizing the area into a grid of elementary point sources; 2) computing the wavefield generated by each point source with a unitary seismic moment; 3) computing seismograms for each point source according to the given distribution of slip; 4) summing up each contribution, synchronized in time, to simulate the propagation of the rupture; 5) adding a stochastic contribution. The basic approach used for computing seismograms in the deterministic low-frequency band is the EXWIM method (Vuan and Priolo, 2003), which simulates the rupture propagation along a finite fault and solves the 3D full-wave propagation in anelastic media with a vertically heterogeneous structure. The computational kernel is the wavenumber integration method (Herrmann and Wang, 1985; Herrmann, 1996a, 1996b). Once seismograms are computed in the low-frequency band, a high-frequency contribution is added. The algorithm works in the frequency domain: first, it defines the amplitude of the high frequency of spectrum through the value of the plateau of the deterministic signal; then it applies a spectral decay according to a pre-assigned attenuation law; hence, it defines the phase spectrum as a random phase; finally, it goes back to the time domain. Special care is taken to avoid the spectral holes in the cross-over band. We model the fault rupture

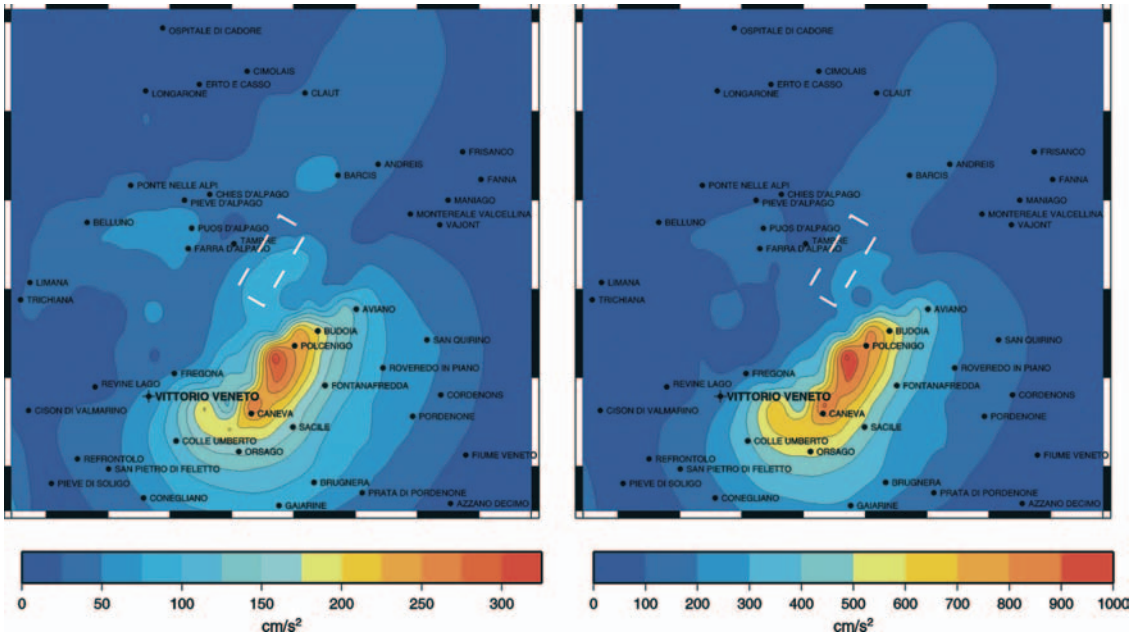

Fig. 6 - *PGA* maps: mean (left) and mean +sd (right) extracted among 480 source nucleation scenarios for the *M*=5.8, October 18, 1936, Cansiglio event. Horizontal component. Dashed line: trace of the rupture plane.

using the kinematic approach by Herrero and Bernard (1994) where the moment density is described by a deterministic-stochastic k^{-2} distribution and an instantaneous slip release. In this study, the rupture propagates from the nucleation point with constant velocity $v_R = 0.8\ v_S$ on the fault plane.

For the low frequency part of the synthetic seismograms, the maximum computational frequency of Green's functions was set at 3 Hz. The high frequency stochastic contribution was added to the final seismogram up to a maximum frequency of about 13 Hz. The deterministic-stochastic cross-over band has been set at 2-3 Hz.

Three different seismic moment distributions and a large number of nucleation points have been considered in order to build an exhaustive set of possible extended source nucleation scenarios. The seismic moment distributions and the location of the 160 nucleation points along the fault plane used for the construction of the scenarios of this study are displayed in Fig. 5.

We show the ground shaking scenario in terms of *PGA*. Fig. 6 shows the maps of the average, and average plus the first standard deviation *PGA* computed for all seismic moment distributions and nucleation points, corresponding to a total of 480 cases. Both maps display a lobe of maximum ground motion south of the source, while the lobe of maximum acceleration resulting from the point source simulations, located north of the epicentre (Fig. 3), is strongly reduced. However, we wish to remind the reader that the scenario displayed in Fig. 6 represents the average of several independent scenarios and does not represent the ground shaking distribution of a single event. In this sense, Fig. 6 should not be compared directly to Fig. 3. Going back to Fig. 6, the area of maximum ground shaking of the mean scenario is located south of Polcenigo, and

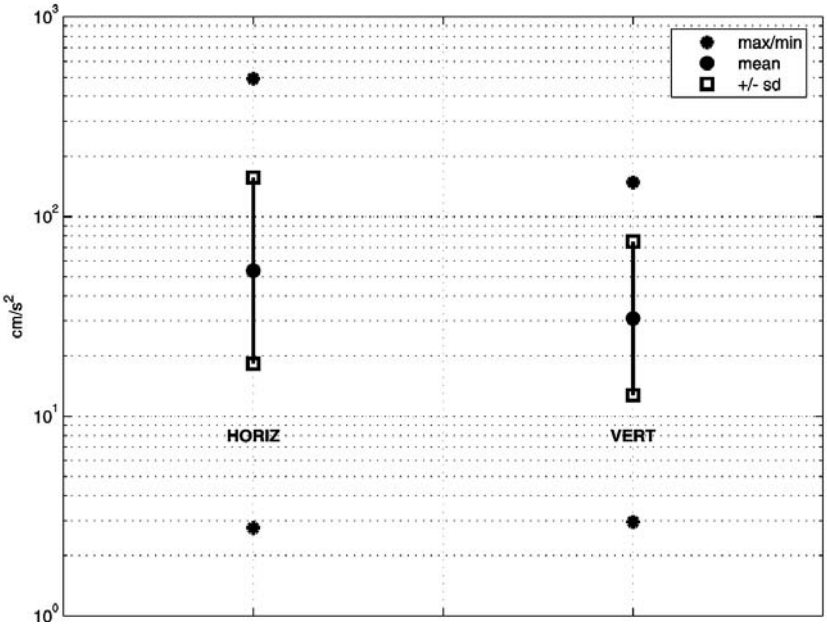

Fig. 7 - *PGA* values estimated at the Vittorio Veneto site for the Cansiglio earthquake by varying the extended source parametrization.

reaches values of about 300 cm/s^2.

The maximum and mean *PGA* with standard deviation (for the horizontal and vertical components) at the Vittorio Veneto site are plotted in Fig. 7. The expected value of the *PGA* at this site is of about 60 cm/s^2 and 30 cm/s^2 for the horizontal and vertical components, respectively. Nevertheless, values of up to three times the average *PGA* still have a large probability of occurrence. As an example, Fig. 8 shows the synthetic seismograms (displacements, velocity and accelerations of the E-W components) computed at Vittorio Veneto for forward and backward directivity conditions (the rupture moves towards the town or away from it, respectively). Note how the direction of rupture propagation strongly influences both amplitude and duration of the estimated ground motion. These examples represent extreme cases which are very rarely observed.

The huge synthetic data set can be further examined by plotting the distribution of the *PGA* values versus distance. Fig. 9 shows the *PGA* values extracted from the seismograms computed at all 441 receivers for all the source hypotheses considered (three seismic moment distributions and 160 nucleation points). The distance goes from the receiver to the fault centre (at a 12 km depth), and varies from 12 km to about 35 km. The maximum *PGA* values are observed at a distance of about 15-20 km. In the same figure, the mean and mean plus/minus the first standard deviation for each receiver are represented by black diamonds, crosses and circles, respectively, while the blue lines represent the best-fit plus/minus the standard deviation, computed considering the whole distribution of values. The ample variability can be noticed: the differences between minimum and maximum values reach three orders of magnitude at some distances.

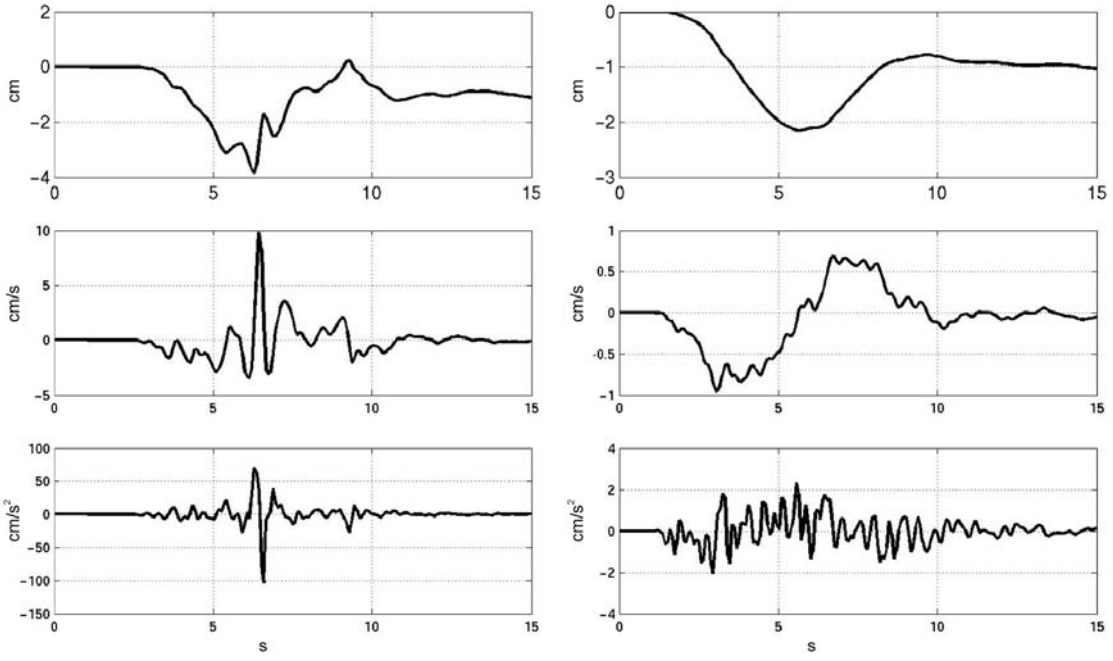

Fig. 8 - Two synthetic seismograms (from top to bottom: displacement, velocity and acceleration of the N-S component) computed at the town of Vittorio Veneto (receiver n. 111 in Fig. 1) for the Cansiglio earthquake with nucleation point located on the fault plane in order to produce the maximum forward (on the left) and backward (on the right) directivity conditions, respectively.

Fig. 9 also shows the 'synthetic' attenuation curves as compared to the attenuation curve by Ambraseys *et al*. (1996) and the curve obtained by Bragato and Slejko (2005), specifically for the eastern Alps within the project. The mean attenuation predicted by this study (blue curve) underestimates the empirical attenuation lines considered. Both empirical curves [magenta coloured by Ambraseys *et al*. (1996) and red by Bragato and Slejko (2005)] fall within the mean and mean plus first standard deviation predicted by this study. In particular, the decay with distance predicted by this study is higher than that predicted by Ambraseys *et al*. (1996), while it is similar to that estimated for the eastern Alps by Bragato and Slejko (2005).

In conclusion, we would like to remark that the synthetic simulations– unlike probabilistic approaches - do provide scenarios which are strongly dependent on the input parameters, such as seismic moment distribution, fault size and rupture nucleation point. The spatial variability exhibited by these kind of scenarios is also strongly dependent on the azimuth. These characteristics can be observed in Fig. 10 which shows the *PGA* maps obtained for the same seismic moment distribution, for four different nucleation points, two with up-dip and two with down-dip rupture direction. Note how, as the nucleation point changes position, the lobe of maximum changes in position as a consequence of the directivity effect.

The wide variability of the predicted *PGA* shows how adequate constraints on the input source parameters to obtain a reliable prediction of the ground motion are needed.

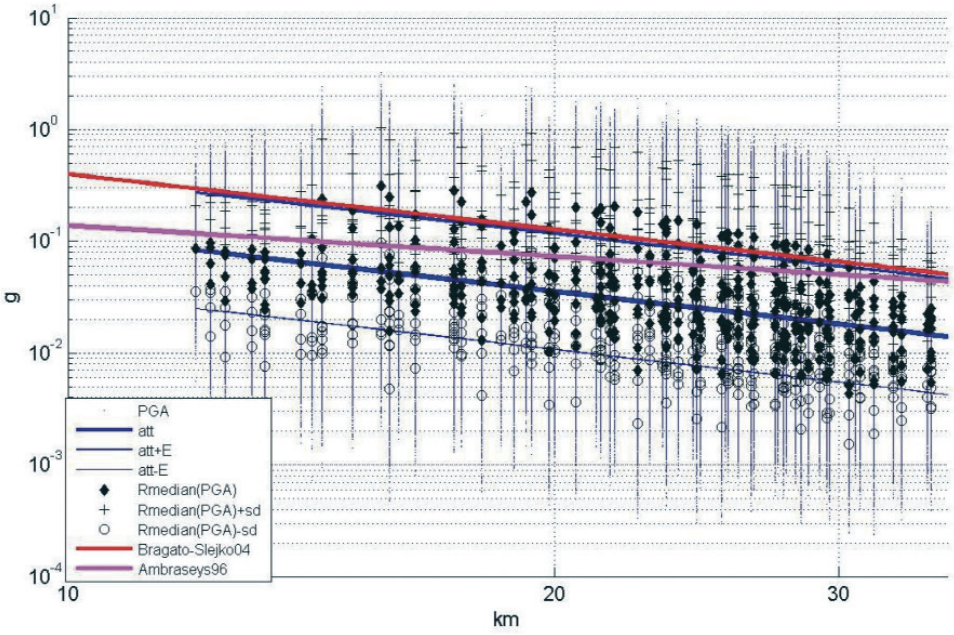

Fig. 9 - Attenuation of the *PGA* values computed in this study (complete synthetic data set, horizontal components) versus the hypocentral distance. Diamonds, plus symbol and circles represent the mean value at each receiver plus/minus the first standard deviation. Blue lines: best-fit obtained considering the whole data set. The thick and thin lines represent the mean and the mean plus/minus the first standard deviation, respectively. Red and magenta line: attenuation curve estimated by the empirical laws of Bragato and Slejko (2005) and Ambraseys *et al.* (1996), respectively.

3. Scenario for the *M*=6.7 Montello earthquake at regional scale

3.1. Study area and structural model

The Montello-Conegliano thrust represents the potentially strongest seismogenic structure known for the area (Galadini *et al.,* 2005). Also in this case, the source parameterization was provided by another project task (Poli *et al*., 2008): the fault plane size is 15 km x 30 km, the estimated magnitude is $M \cong 6.7$ (Wells and Coppersmith, 1994) and the fault mechanism is mainly reverse ($\phi = 240°$, $\delta = 30°$, $\lambda = 110°$). The fault dips towards NW from 3 km to about 12 km of depth. The study area (Fig. 11a) is a square with a 35 km side centred at the epicentre of the reference earthquake, and is sampled by 121 receivers, inter-spaced by 3.5 km.

Similarly to the simulations performed for the *M*=5.8 October 18, 1936 Cansiglio event, we adopted different structural models for receivers located in the areas corresponding to different structural compartments, where the surface geology has also been taken into account in a simplified way. Three different structural, plane-layer models have been defined for each structural compartment using the information given by the available geological sections of the study area (Fig. 11). For the compartments corresponding to the Veneto Plain and piedmont area, indicated with p2 and p1 in Fig. 11a respectively, a surface layer representing the Quaternary soils was added at the top of the 1D models. For this layer, the shear wave velocity is 1.1 km/s, and the thickness is 50 m and 150 m for models p1 and p2, respectively.

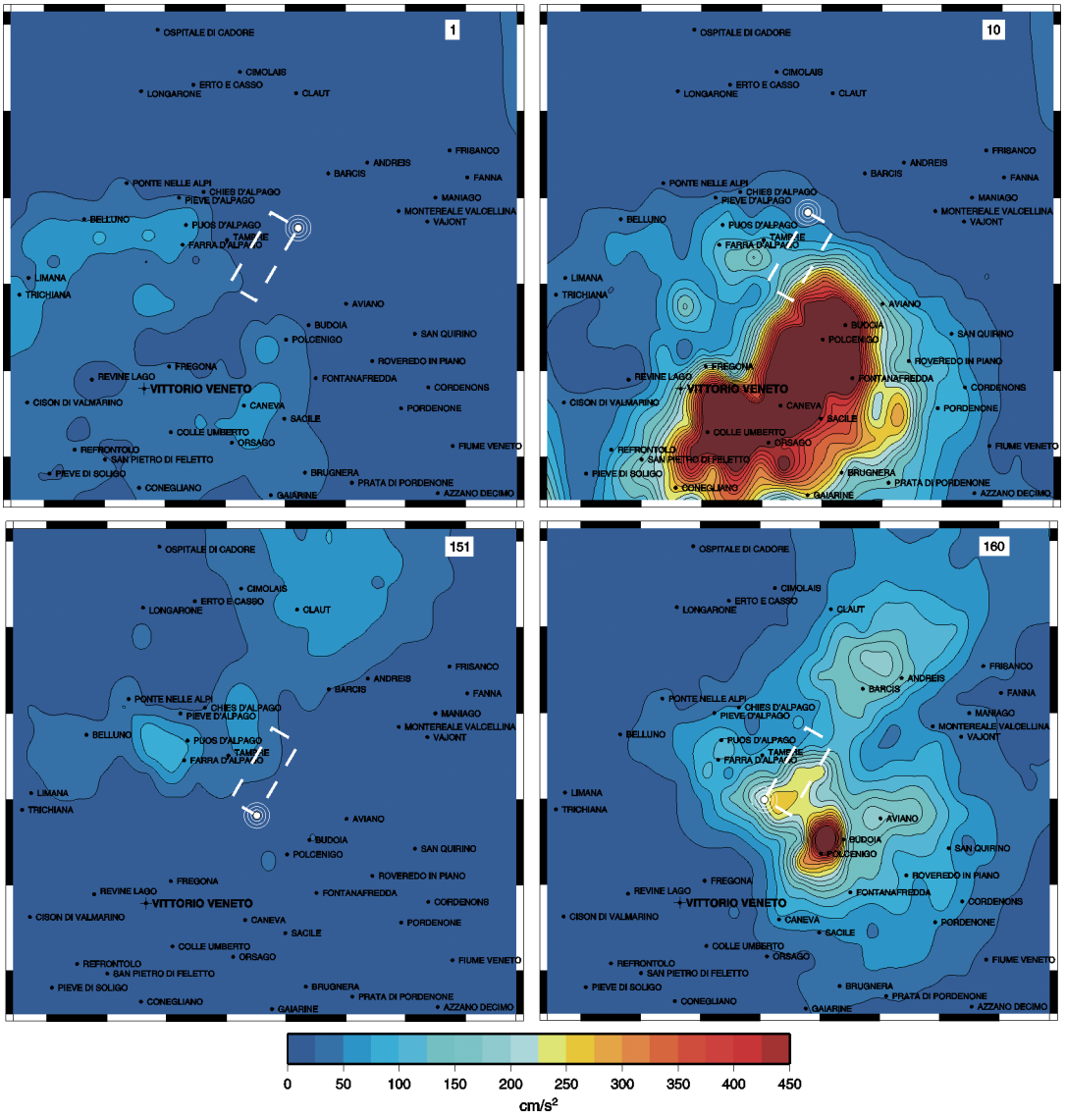

Fig. 10 - *PGA* maps (horizontal component) computed for different nucleation points.

3.2. Extended source simulations

The modelling procedure is very similar to that used for modelling the Cansiglio events, i.e., seismograms are obtained by the hybrid stochastic-deterministic EXWIM technique. Nevertheless, the overall computational efficiency has been improved through the use of harmonic interpolation (Vuan and Priolo, 2003). In this way, the number of basic seismograms was reduced from about 12,000 to about 3,000. Deterministic seismograms were computed up to 3 Hz, and the stochastic contribution was added to the maximum frequency of 13.3 Hz, with the cross-over band of the deterministic-stochastic transition set at 2.0-3.0 Hz. In order to build an

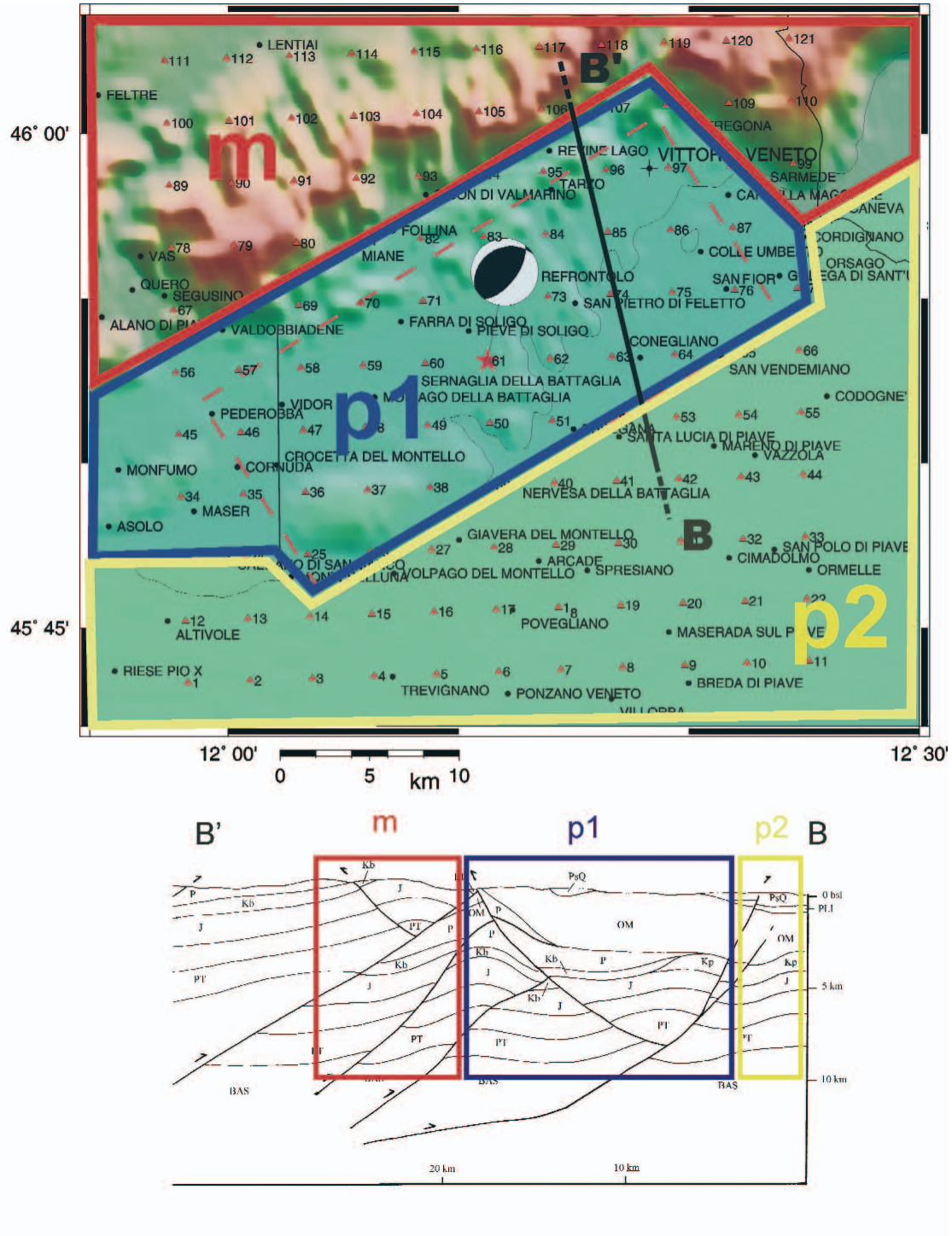

Fig. 11 - (a) Map showing the study area, receiver location and fault geometry. The areas corresponding to the three different structural models are also shown. (b) Geological section B-B' used in the definition of the three-plane layer models.

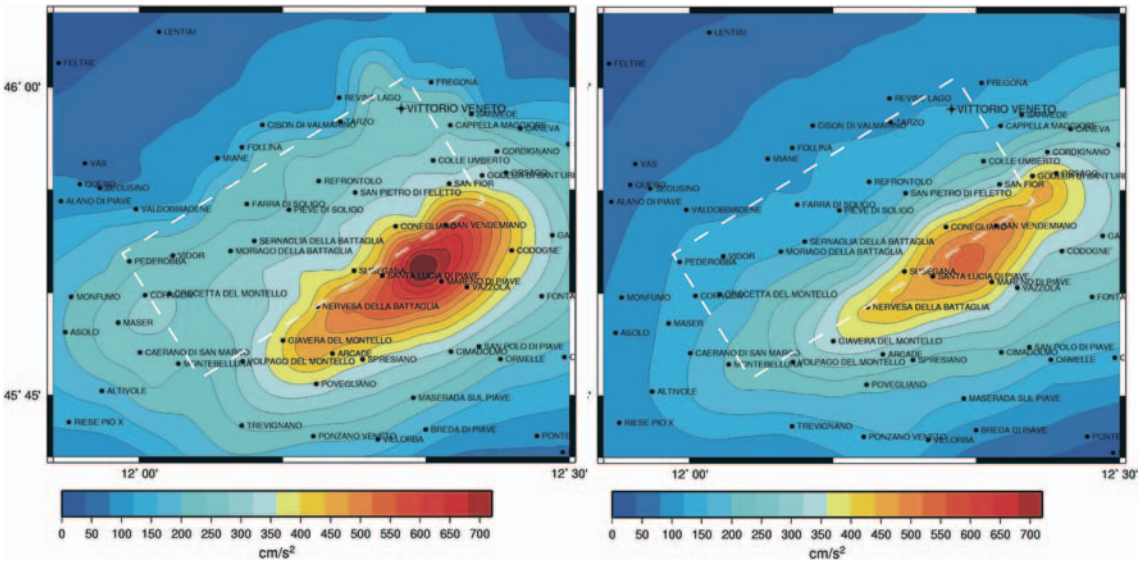

Fig. 12 - Mean *PGA* extracted among 1014 source nucleation scenarios for a hypothetical *M*=6.7 Montello earthquake. Horizontal (left) and vertical (right) component. Dashed line: trace of the rupture plane.

exhaustive set of possible scenarios, we have considered three different seismic moment distributions and a grid of 338 nucleation points (i.e. hypocentre locations) located along the fault segment for a total of 1014 source activation scenarios.

Fig. 12 shows the mean *PGA* scenario computed for the horizontal and vertical components. The maximum *PGA* values for the mean scenario correspond to the area of hypothetical

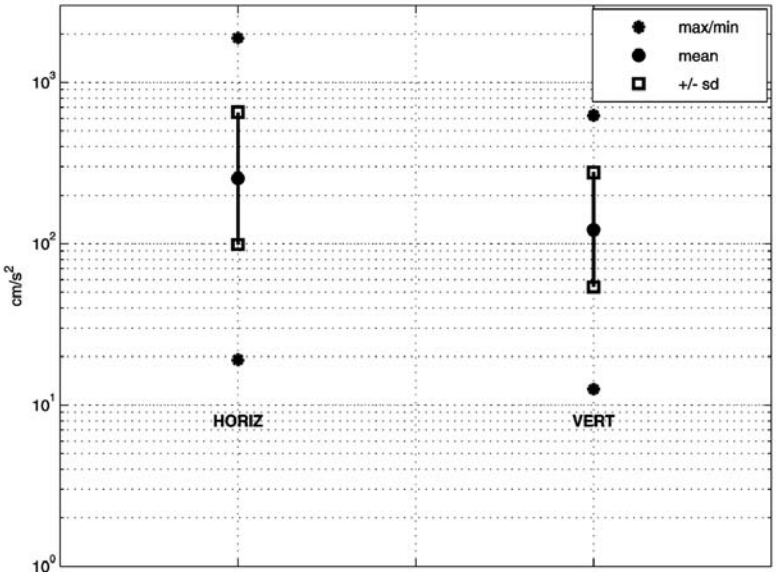

Fig. 13 - *PGA* values obtained at the Vittorio Veneto site for the Montello earthquake.

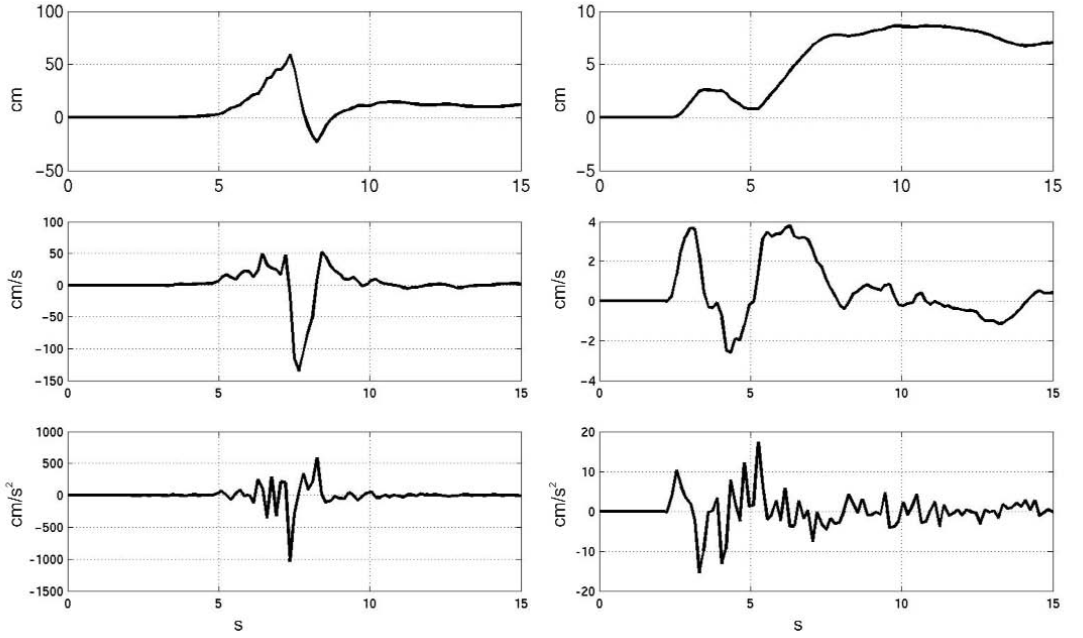

Fig. 14 - Two synthetic seismograms (from top to bottom: displacement, velocity and acceleration of the N-S component) computed at the town of Vittorio Veneto (receiver n. 97 in Fig. 11) for the Montello earthquake with nucleation point located on the fault plane in order to produce the maximum forward (on the left) and backward (on the right) directivity conditions, respectively.

outcropping of the fault plane, near the villages of Santa Lucia di Piave and Mareno di Piave. Here, the estimated *PGA* is about 0.7 g. Fig. 13 shows the maximum and mean *PGA* with standard deviation (for both horizontal and vertical components) estimated at the Vittorio Veneto site (receiver number 97, in Fig. 11a). The *PGA* expectation values at this site are of about 250 cm/s^2 and 120 cm/s^2 for the horizontal and vertical components, respectively. A wide variability of the values, similar to the *M*=5.8 Cansiglio event scenarios can be noticed.

Fig. 14 shows two examples of seismograms computed at Vittorio Veneto, with relatively high (left panel) and low (right panel) *PGA* values. They correspond to forward and backward directivity conditions, respectively. The apparent short duration of the seismograms on the left panel of Fig. 14 is explained by the directivity effect and by the low dispersion of the seismic waves because of the very near filed conditions. Moreover, because of the simplicity of the 1D model, no coda is generated by scattering.

The distribution of the synthetic *PGA* values versus hypocentral distance is shown in Fig. 15. The distance varies from 7.5 km (site above the fault centre) to about 26 km. As in the Cansiglio scenario case, the maximum *PGA* values occur between 15 and 20 km, rather than at the minimum distance. The comparison of the synthetic attenuation curves with the empirical attenuation curves by Ambraseys *et al*. (1996) and Bragato and Slejko (2004), respectively, shows that the first one (magenta line) slightly underestimates the mean attenuation predicted by this study, while the second one (red line) nearly fits the mean *PGA* plus the first standard deviation.

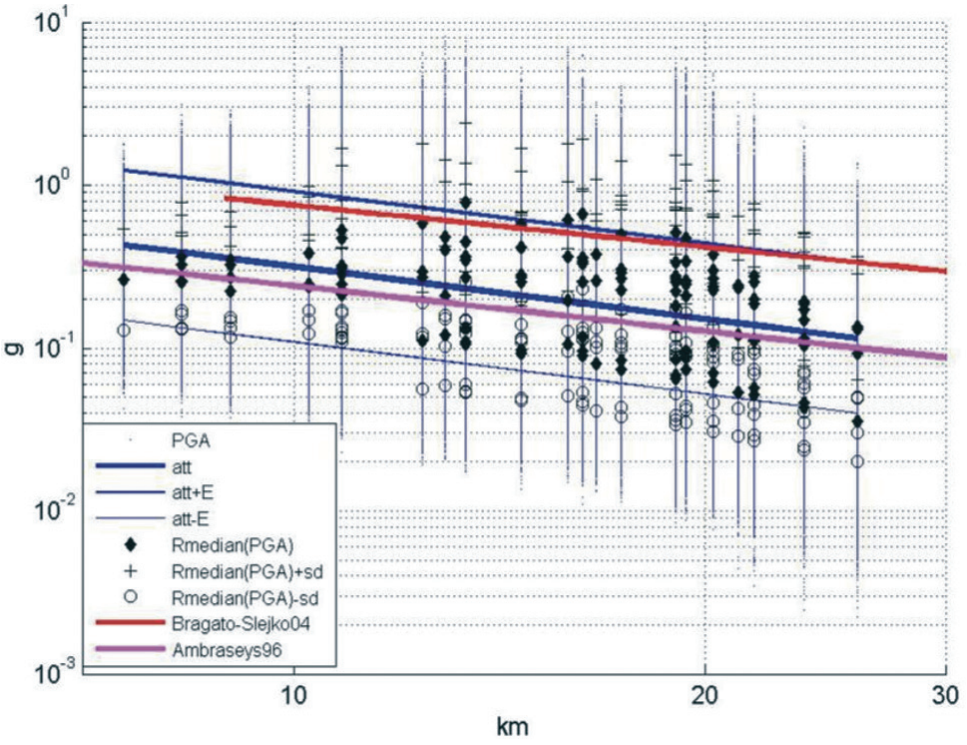

Fig. 15 - Attenuation of the *PGA* values computed in this study (complete synthetic data set, horizontal components) versus the hypocentral distance. Other details as in Fig. 9.

The decay with distance of the synthetic attenuation curves is a little larger than that displayed by the two empirical laws. The same large variability already observed for the *M*=5.8 Cansiglio event scenarios can be noticed.

4. Detailed scenarios for the *M*=5.8 Cansiglio earthquake

In order to understand the effect on the ground motion of the wave-field propagation through the complex geological structure of the Alpago-Cansiglio for the area of Vittorio Veneto, a specific study has been performed using the 2D spectral element method (SPEM 2D). The 2D spectral element method (SPEM 2D), solves the seismic wave propagation through complex geological structures and allows us to estimate the effects of a deep crustal structure, surficial geology and topography on the ground shaking. All the information available today has been collected and used to build up the most realistic structural models for the study area.

Here, we describe the results of the numerical simulations performed using the *M*=5.8, October 18, 1936, Cansiglio event as a reference earthquake, and for a transect (i.e., a 2D vertical plane) NE-SW oriented, which crosses the centre of Vittorio Veneto directly south of Serravalle, i.e. right across the area of the present expansion of the city (Fig. 16). The results of the simulations are analyzed using snapshots of the wave field propagation as well as complete

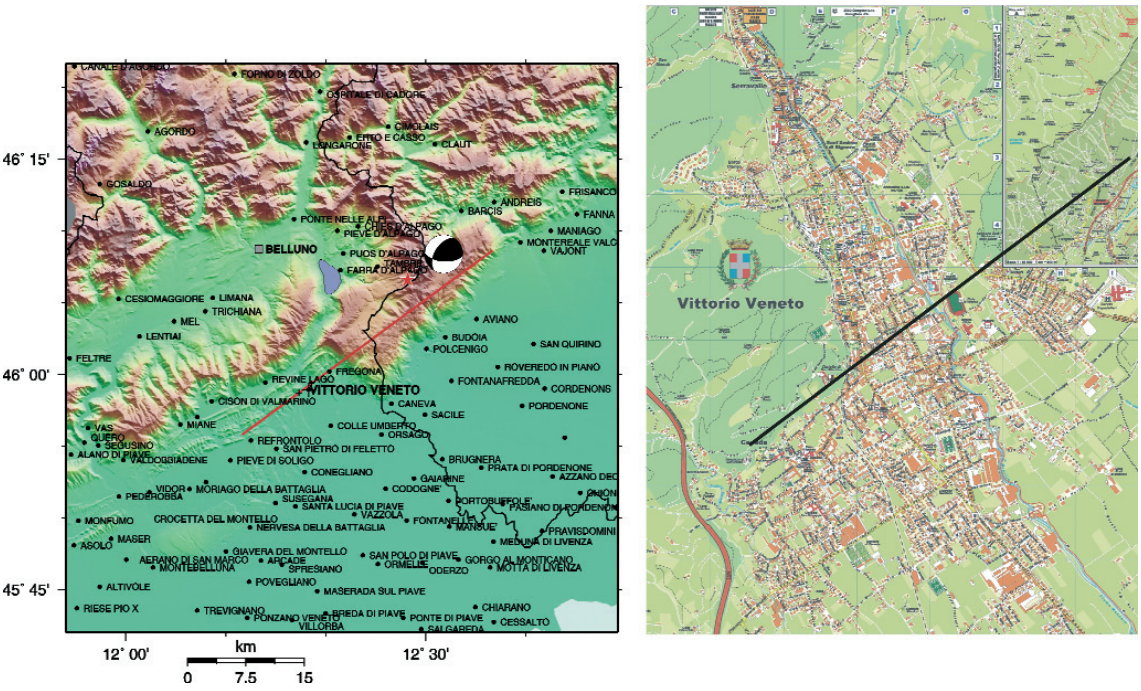

Fig. 16. Left panel: map of the study area showing the location of the transect for which the structural model (red line) has been defined. The epicenter of the *M*=5.8, October 18, 1936, Cansiglio event is indicated by the red star. Right panel: location of the transect across the Vittorio Veneto area.

synthetic waveforms at the model surface.

4.1. Model and source parameterization

The Chebyshev spectral element method (SPEM) is a high-order finite element technique, which solves the variational formulation of the elasto-dynamic equation. This approach provides accurate solutions of the full wave field propagation, that includes converted body waves and surface waves, and allows for an accurate description of the medium heterogeneity at several scale lengths. The computational domain is decomposed into non-overlapping, quadrilateral elements, and then, the solution of the variational problem is expressed on each element, as a truncated expansion of Chebyshev orthogonal polynomials, as in the spectral methods. More details on the application of the 2D Chebyshev SPEM to the simulation of the seismic ground motion induced by earthquakes can be found in Priolo (2001, 2003).

The construction of a geological model was carried out with the contribution of the geologists of the University of Udine. The model (Fig. 17) is characterized by a compressive structure, running at the base of the Cansiglio Massif and superimposing the Mesozoic carbonatic platform sequence on the Tertiary terrigenous sequence. This model specifies the local shallow geological structure and topography in detail in the Vittorio Veneto area (Fig. 18). In this part, the Quaternary sediments are formed by alluvial and glacial deposits about 70 m thick, with the presence of local lenses of sand and conglomerates which are not reproduced in the model. The

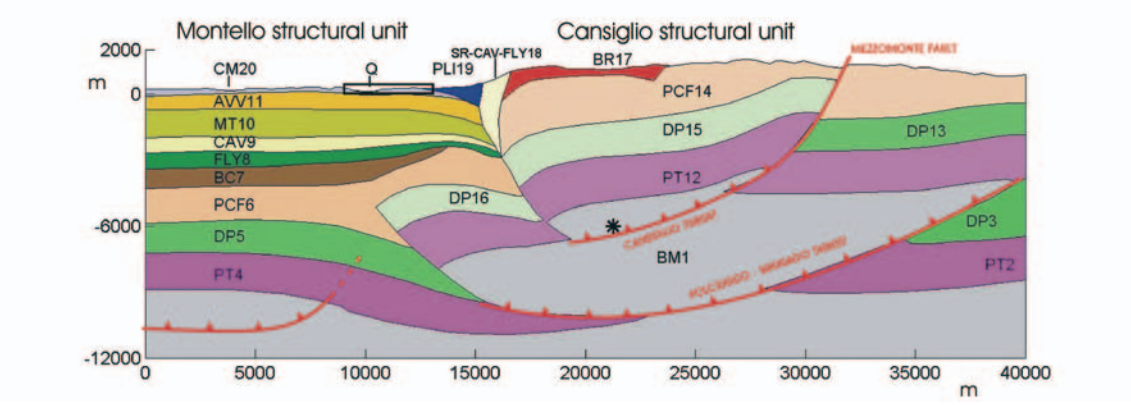

Fig. 17 - Computational model of the modelled transect. Different colours indicate regions with homogeneous properties inside. The physical properties for each region are indicated in Table 1.

geological structure is represented as a patch of regions, or sub-domains, which are related to the lithologies. Each sub-domain is discretized into homogenous elements. In each element, rock formations and soils are expressed in terms of body waves velocities, density and attenuation. Figs. 17 and 18 show the structural model divided into sub-domains and a zoom in the Vittorio Veneto area along the modelled transect, respectively.

The source is simulated through a point shear dislocation (double-couple model). The source time history is obtained as a summation of two pulses, characterized by distinct corner frequencies f_c and f_{asp}, which represent the inverse of the average rupture duration of the whole source area (RA) and the largest asperity area (RA_{asp}), respectively. Estimating the average slip duration as $T_S \approx \frac{2\sqrt{S}}{3V_r}$ (Heaton, 1990), where S and V_r are the rupture area and velocity, respectively, and the ratio between the total rupture area and that of the largest asperity is $RA_{asp} \approx 17.5\%\ RA$ (Somerville *et al.*, 1999), it transpires that the ratio between the two corner frequencies can be approximated by $f_{asp} \approx 2.4\, f_c$. Therefore, if we assume that $f_c = 0.6$ Hz

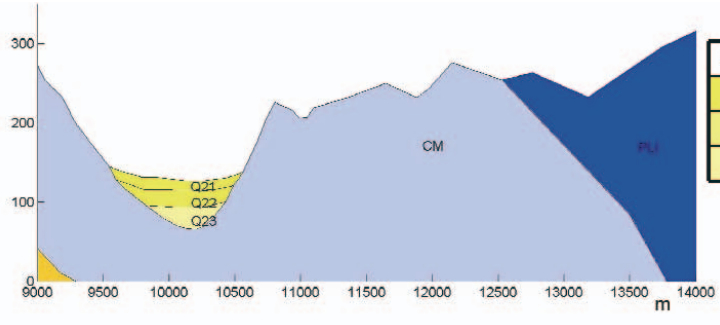

Abbrev.	V_p(m/s)	V_s(m/s)	ρ(g/m^3)	Q
Q21	1800	900	1900	80
Q22	2400	1400	2000	100
Q23	3000	1700	2100	100

Fig. 18 - Detailed structure defined for the sedimentary basin of Vittorio Veneto along the transect.

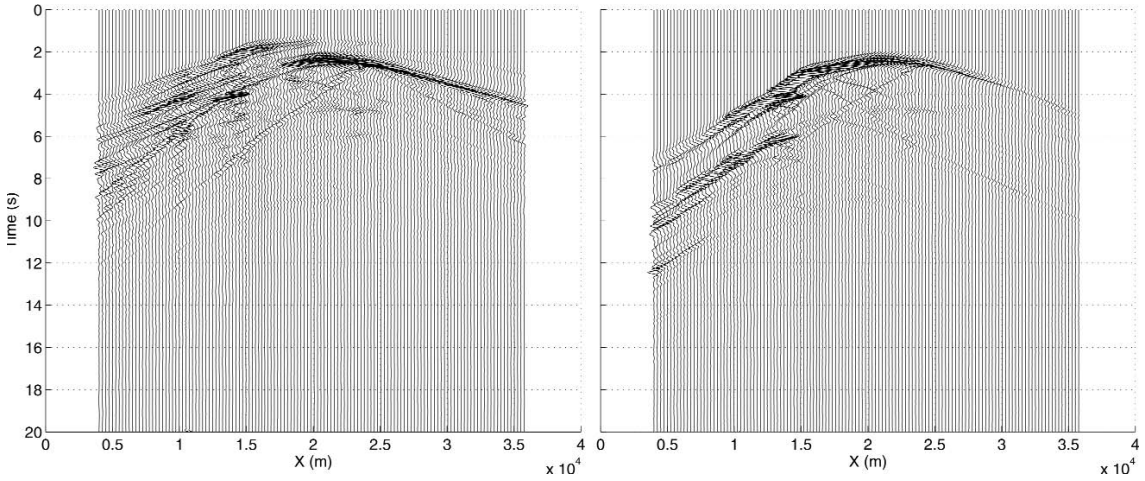

Fig. 19 - Acceleration seismograms computed at the surface of the transect, with receiver inter-spacing of 25 m. Radial (left panel) and transversal (right panel) components. Coordinates correspond to those of the structural model specified in Fig. 17.

Table 1 - Physical properties of the rock materials that define the 2D transect of Fig. 17.

Abbrev.	Geological formation	V_p(m/s)	V_s(m/s)	ρ(g/m^3)	Q
PLI	Conegliano Complex	3200	1850	2000	120
SR	Scaglia Rossa fm.	4000	2310	2300	120
BR	Fadalto Limestone	4500	2600	2400	140
CM	Montello Conglomerate	4000	2310	2300	120
AVV	Vittorio Veneto Sandstone (Tortonian)	3200	1850	2100	120
MT	Tarzo Marl (Serravallian)	3000	1730	2000	110
CAV	Cavanella Group (Cattian-Langhian)	4000	2300	2200	120
FLY	Belluno Flysh	3500	2020	2100	150
BC	Biancone - Soverzene	4000	2310	2300	120
PCF	Platform Carbonates (Jurassic-Cretaceous)	6000	3470	2600	200
DP	Dolomia Principale (upper Triassic)	6500	3760	2700	230
PT	Permian Triassic undifferentiated Complex	5500	3180	2300	160
BM	Basement	6000	3470	2600	200

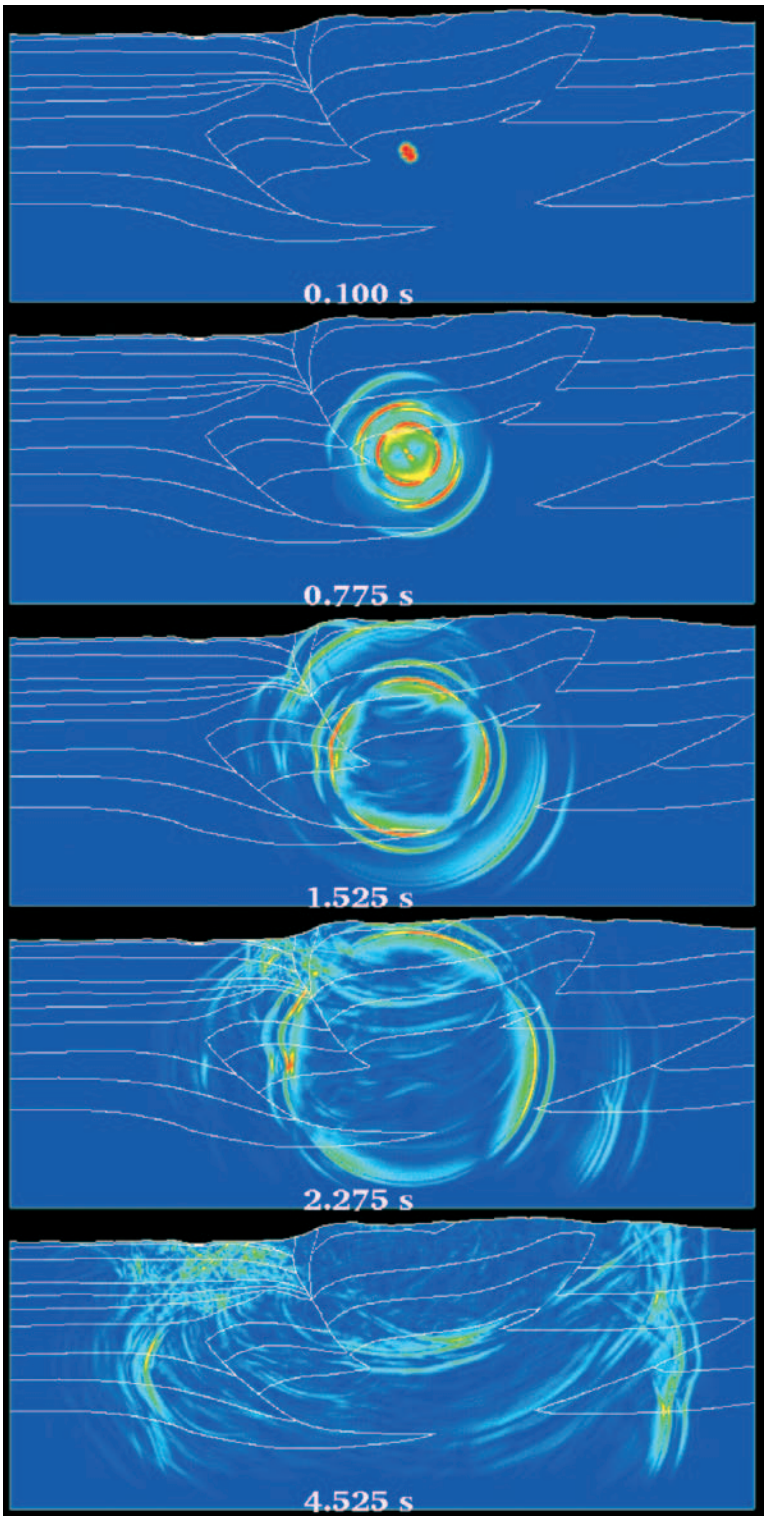

Fig. 20 - Snapshots of the acceleration wavefield (amplitude) at different propagation times. The wavefield is attenuated by the presence of absorbing strips at the model boundary. Note that each wavefront consists of a double pulse, as a result of the shape of the source time history. See text for further details.

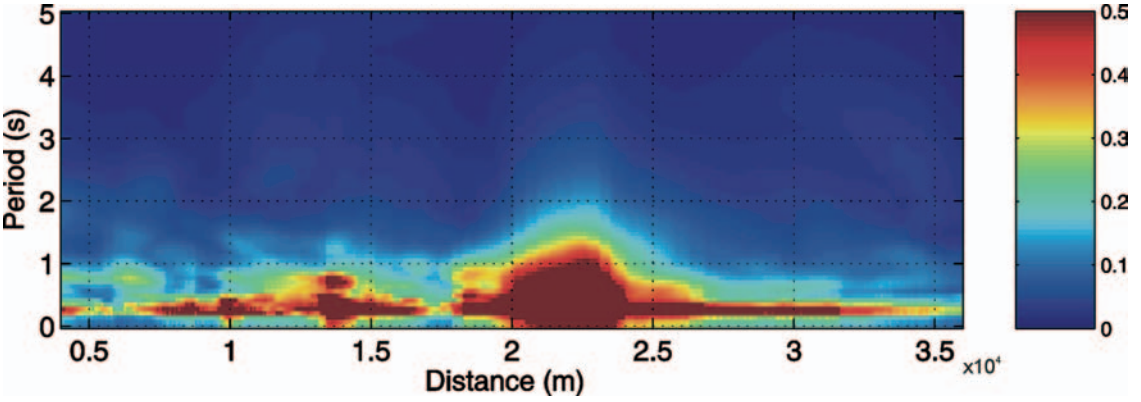

Fig. 21 - Surface distribution of acceleration response spectra (5% damping). Horizontal radial component.

(Heaton, 1990), it results that $f_{asp} \approx 1.4$ Hz. The amplitude of the computed wave field is scaled by the value of the average slip at the source. We have estimated a value of $D = 21$ cm (Kanamori and Anderson, 1975) and $D_{asp} \approx 2.01\ D$ (Somerville *et al.*, 1999) = 42 cm for the average slip associated to the whole fault segment and asperity, respectively.

4.2. 2D simulations

Fig. 19 shows the acceleration seismograms computed at the surface of the transect for the radial (P-SV) and transversal (SH) components, respectively. The town of Vittorio Veneto is located between abscissas 9500 m and 10600 m. In spite of the rather complex waveform pattern, both P and S direct arrivals can be clearly recognised at times of about 1.3 s and 2.0 s, respectively. Surface waves can also be recognized: they are generated either by the impact at the surface of the direct wave field that propagates vertically from the source (see for instance at an abscissa of about 24 km, which corresponds to the Cansiglio region) or by the topographical relief corresponding to the Cansiglio escarpment, at an abscissa of about 15 km. Note that the surface wave velocity varies across the model according to the S-wave velocity of the different

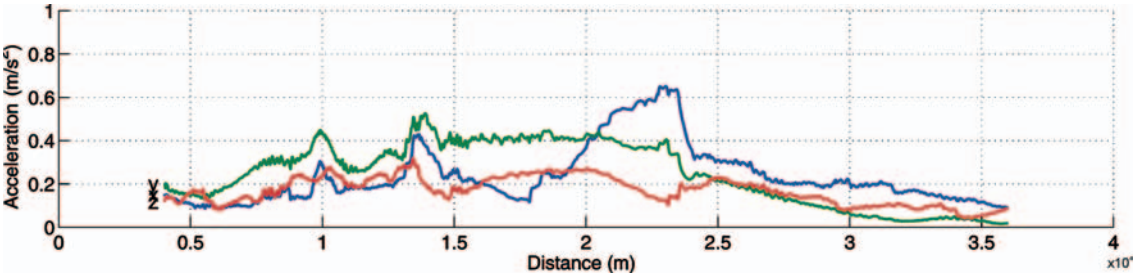

Fig. 22 - Surface distribution of *PGA*. The blue, the green and the red indicate, radial, transversal, and vertical components, respectively.

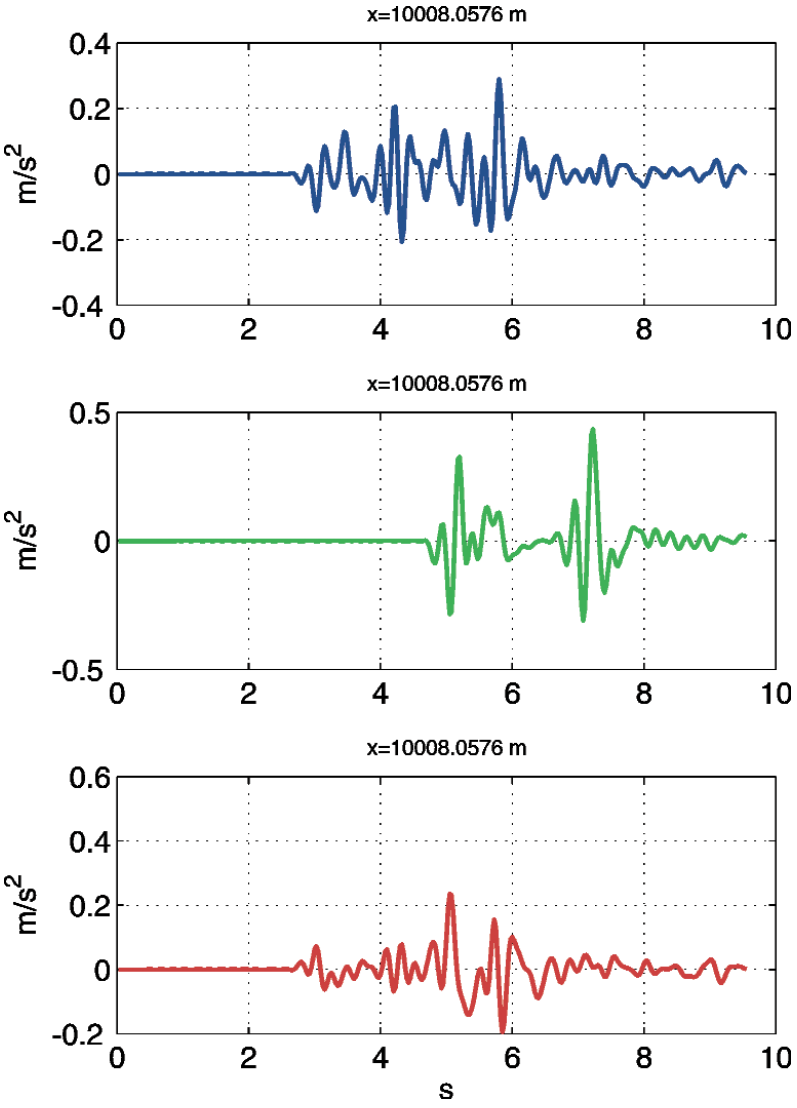

Fig. 23 - Acceleration computed at a receiver in the Vittorio Veneto basin. From top to bottom: radial, transversal and vertical component.

lithologies. In particular, the velocity is higher along the Cansiglio structural unit (in Fig. 17, unit PCF at x < 16 km, with Vs=3470 m/s), while it is lower toward SW along the Montello structural unit (units CM, AVV, and MT, with Vs < 2000 m/s).

Looking at the sequence of the wavefield acceleration snapshots of Fig. 20 can give a more complete interpretation. Here, we can easily identify the direct P and S wavefronts, the head waves, the wave conversions generated at structure interfaces, and the surface waves which propagate along the surface. Note in particular: 1) how the SV-lobe which propagates into the Montello structure is deviated upwards by the fault that separates the Cansiglio and Montello structural units; and 2) the complexity of the wavefield through the Montello structural unit as an effect of the multilayered structure.

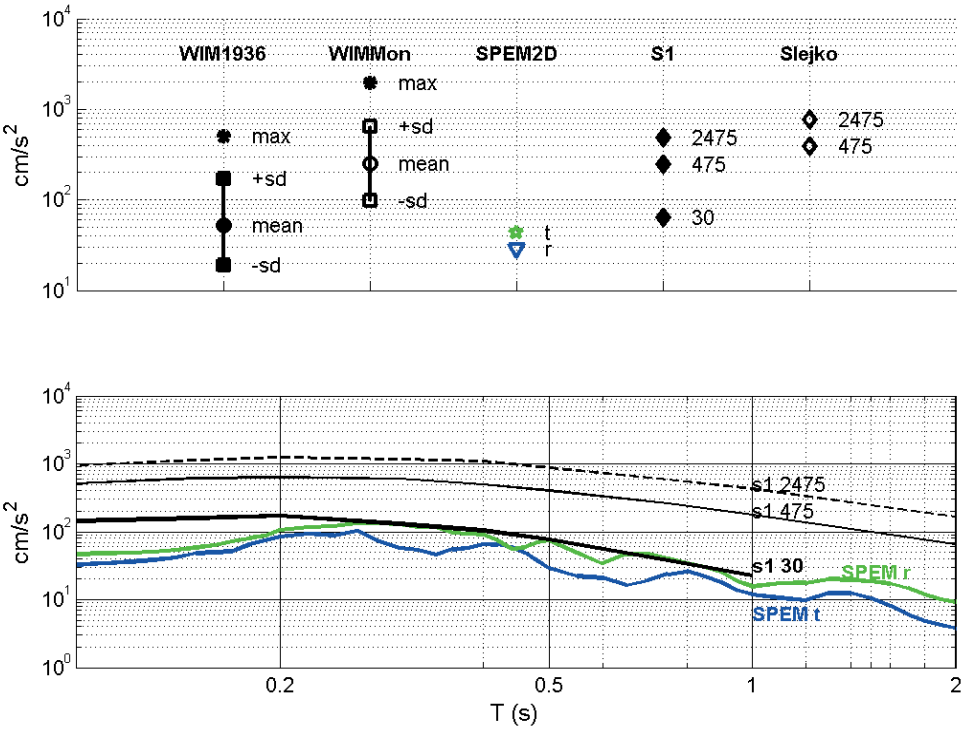

Fig. 24 - Top panel: *PGA* values obtained at the Vittorio Veneto site by EXWIM (horizontal component computed for the Cansiglio and Montello reference earthquakes, respectively), SPEM 2D (radial and transversal components) and the values (S1) provided by the new seismic hazard reference map (Meletti and Montaldo, 2007) for the probability of exceedance in 50 years of 81%, 10 % and 2%, corresponding to a return period of 30, 475 and 2475 respectively, and by Slejko *et al.* (2008) for the return period of 475 and 2475. Bottom panel: acceleration response spectra computed by SPEM 2D (radial and transversal components) at the Vittorio Veneto site and those obtained by Montaldo and Meletti (2007) for the construction of the seismic hazard maps of spectral acceleration.

Figs. 21 and 22 show the distribution of the horizontal acceleration response spectra (radial component) and the *PGA* (all components) at the transect surface. We can clearly distinguish three areas of large amplitude. The largest values occur at the surface of the Cansiglio structural unit (20 km < x < 24 km, in Fig. 17), right above the source position, and are due to the arrival of a direct SV-wavefront. Note that the vertical component has a minimum in this area. Here, the acceleration response spectra show the maximum amplitude in the band (0.5 to 4.5 Hz). A second area is at the abscissa between 12.5 km and 15 km. It corresponds to the arrival of another direct SV-wavefront, which has been deviated by the geological structure. In this area, the acceleration response spectra show the maximum energy in the band (1.0 Hz, 4.5 Hz). The third area corresponds to the Vittorio Veneto basin (9.5 km < x < 10.5 km). Here, the large amplitude is a site effect generated by the seismic energy trapped within the low velocity quaternary deposits, and the energy is concentrated in a narrower band between 2 Hz and 4.5 Hz.

Fig. 23 shows a sample of synthetic seismograms computed in the middle of the Vittorio Veneto basin (x < 10 km). The presence of multiple reflections, due to the wave field being trapped in the surficial deposits, can be observed. The *PGA* values predicted for the radial,

transversal and vertical components are about 0.3, 0.45 and 0.2 m/s^2 at Vittorio Veneto and 0.65, 0.4 and 0.2 m/s^2 in the area of maximum ground motion (x < 23 km), respectively.

Fig. 24 (top panel) summarizes the results obtained by the two different techniques (i.e., the EXWIM and SPEM 2D) in terms of *PGA* at the Vittorio Veneto site and compares them to the *PGA* for different probabilities of exceedance provided by the new seismic hazard reference map (Montaldo and Meletti, 2007) and that computed by Slejko *et al*. (2008). It can be seen that the mean value obtained by the EXWIM simulation for the Cansiglio reference earthquake (which is a medium-sized earthquake for this area) is comparable with the *PGA* with 81% of probability of exceedance in 50 years (corresponding to a return period of 30 years), while the maximum value obtained for the same reference event is comparable to a *PGA* of 2% of probability of exceedance in 50 years (return period of 2475). On the other hand, the mean value obtained by EXWIM for the Montello reference earthquake (which is considered the maximum credible earthquake) is comparable with the *PGA* corresponding to a return period of 475 years. It can be noticed that the *PGA* value obtained by SPEM 2D for the Cansiglio event at the Vittorio Veneto site falls in the range between the mean and the mean less one standard deviation predicted by the EXWIM simulation. The response spectra computed for the two horizontal components (coloured lines in the bottom panel of Fig. 24) with the SPEM 2D simulation at Vittorio Veneto are comparable with the spectral acceleration with a return period of 30 years (Montaldo and Meletti, 2007) for the periods between 0.2 and 1 second.

5. Conclusions

The goal of this study is to estimate the ground motion in the town of Vittorio Veneto and its neighbouring area by taking into account some physical elements, explicitly not considered by classical approaches, such as the effect of the structural geophysical model, the finiteness of the earthquake source, and the full-wave propagation of the seismic wavefield radiated from the source. To this aim, two different techniques have been used.

The first method, EXWIM, computes the ground motion for extended source models, where the kinematics of rupture propagation is prescribed. With this method, we have analyzed the sensitivity of the estimations to the variation of some random parameters, such as the seismic moment distribution and the hypocentral location. Two possible seismic sources have been chosen as a reference earthquake. The first is associated to the Cansiglio-Alpago structure, representing the 1936 earthquake (M=5.8); the second represents a hypothetical earthquake associated with the Montello thrust, which was identified as one of the major potential seismogenic structures of the region. The results obtained for the Cansiglio earthquake with this approach are consistent, on average, with those obtained by classical approaches (reference to Slejko *et al.*, 2008), notwithstanding a high variability feature for what concerns both the spatial distribution and the statistical properties. Thus, the importance of providing as many constraints as possible, for the source parameterization in order to obtain reliable predictions of ground motion, emerges.

The second method used in this study is the 2D spectral elements method (SPEM 2D). It has been used to evaluate the effects of the complex geological structure of the study area on the town of Vittorio Veneto. The reference earthquake was the 1936 Cansiglio event. The results show that the combined effect of the source radiation pattern and wave-field propagation through the

geological structure strongly influences the ground-shaking distribution along the 2D transect. The Vittorio Veneto area corresponds to a zone of relative minimum ground motion for the 1936, Cansiglio earthquake, thus confirming the EXWIM scenario indications. However, the *PGA* and all other ground motion indices feature a local rise at the Vittorio Veneto basin, which is caused by seismic energy trapped within the lower velocity soils of the valley. This suggests how important it is to consider the site effects as a key factor when assessing the seismic hazard in the town of Vittorio Veneto.

Acknowledgements. This work was funded by the National Group for the Defence Against Earthquakes (GNDT), under the project 'Scenarios of seismic damages in Friuli and Veneto'. We would like to thank: M. Eliana Poli for the definition of both the 1D and 2D structural models of the investigated area and the source parameterization of the Montello reference earthquake; G. Bressan for the definition of the 1D average geological structures and the source parameterization for the Cansiglio reference earthquake; A. Vuan and P. Klinc for the valuable discussions and suggestions. The maps of Figs. 1, 2, 3, 4, 6, 10, 11, 12 and 16 were created by GMT software (Wessel and Smith, 1995).

REFERENCES

Ambraseys N.N., Simpson K.A. and Bommer J.J.; 1996: *Prediction of horizontal response spectra in Europe.* Earthquake Engineering & Structural Dynamics, **25**, 371-400.

Boschi E., Guidoboni E., Ferrari G., Valensise G. and Gasperini P. (eds); 1997: *Catalogo dei forti terremoti in Italia dal 461 a.C. al 1990*. 2, ING-SGA, Bologna, 644 pp.

Bragato P. L. and Slejko D.; 2005: *Empirical ground motion attenuation relations for the eastern Alps in the magnitude range 2.5-6.3*. Bull. Seis. Soc. Am., **95**, 252-276.

Galadini F., Poli M.E. and Zanferrari A.; 2005: *Seismogenic sources potentially responsible for earthquakes with M ≥ 6 in the eastern Southern Alps (Thiene-Udine sector, NE Italy)*. Geophys. J. Int, **161**, 739-762.

Hanks T. C. and Kanamori H.; 1979: *A moment-magnitude scale*. J. Geophys. Res., **84**, 2348-2350.

Heaton T. H.; 1990: *Evidence for and implications of self-healing pulses of slip in earthquake rupture.* Phys. Earth Planet. Inter., **64**, 1-20.

Herrero A. and Bernard P.; 1994: *A kinematic self-similar rupture process for earthquakes.* Bull. Seism. Soc. Am., **84**, 1216-1228.

Herrmann R. B. and Wang C. Y.; 1985: *A comparison of synthetic seismograms*. Bull. Seism. Soc. Am., **75**, 41-56.

Herrmann R. B.; 1996a: *Computers program in seismology. An overview of synthetic seismogram computation.* Dep. of Earth and Atmospheric Sciences; Saint Louis University. Version 3.0 edition.

Herrmann R. B.; 1996b: *Computers program in seismology. Volume VI: wavenumber integration*. Dep. of Earth and Atmospheric Sciences; Saint Louis University. Version 3.0 edition.

Kanamori H. and Anderson L.; 1975: *Theoretical basis of some empirical relations in seismology.* Bull. Seism. Soc. Am., **65,** 1073-1095.

Marcellini A.; 1995: *Arrhenius behavior of aftershock sequences*. Journ. Geophys. Res., **100**, 6463-6468.

Meletti C. and Montaldo V.; 2007: *Stime di pericolosità sismica per diverse probabilità di superamento in 50 anni: valori di ag*. Progetto DPC-INGV S1, http://esse1.mi.ingv.it/d2.html.

Montaldo V. and Meletti C.; 2007: *Valutazione del valore della ordinata spettrale a 1sec e ad altri periodi di interesse ingegneristico.* Progetto DPC-INGV S1, http://esse1.mi.ingv.it/d3.html.

Pettenati F. and Sirovich L.; 2003: T*ests of source-parameter inversion of the U.S. Geological Survey intensities of the Whittier Narrows, 1987 earthquak*e. Bull. Seism. Soc. Am., **93**, 47-60.

Poli M.E., Burrato P., Galadini F. and Zanferrari A.; 2008: *Seismogenic sources responsible for destructive earthquakes*

in north-eastern Italy. Boll. Geof Teor. Appl., **49**, 301-313.

Priolo E.; 2001: *Earthquake ground motion simulation through the 2-D spectral element method.* J. Comp. Acoustics, **9**, 1561-1581.

Priolo E.; 2003: *Ground motion modelling using the 2-D Chebyshev Spectral Element Method.* In: Bull J.W. (ed), Numerical Analysis and Modeling in Geomechanics, Spon Press Taylor and Francis Group Ltd., London, 371 pp.

Slejko D., Rebez A. and Santulin M.; 2008: *Seismic hazard estimates for the Vittorio Veneto broader area (NE Italy).* Boll. Geof. Teor. Appl., **49**, 329-356.

Somerville P., Irikura K., Graves R., Sawada S., Wald D., Abrahmson N., Iwasaki Y., Kagawa T., Smith N. and Kowada A.;1999: *Characterizing crustal earthquake slip models for the prediction of strong ground motion.* Seism. Res. Lett., **70**, 59-80.

Vuan A. and Priolo E.; 2003: *Harmonic interpolation for multiple source simulations in a vertically varying media*. In: Cocco M. (ed), Development and comparison between methodologies for the evaluation of seismic hazard in seismogenetic areas: application to the Central and Southern Apennines, Second year activity report, UR2 TASK4. GNDT 200-2002.

Wells D. and Coppersmith K.; 1994: *New empirical relationships among amplitude, rupture length, rupture width, rupture area, and surface displacement*. Bull. Seism. Soc. Am., **84**, 974-1002.

Wessel P. and Smith W. H. F.; 1995: *New version of the Generic Mapping Tools, EOS Trans*. Am. Geophys. Union, **76**, 329 pp.

Corresponding author: Giovanna Laurenzano
Dipartimento Centro di Ricerche Sismologiche
Istituto Nazionale di Oceanografia e di Geofisica Sperimentale
Borgo Grotta Gigante 42/c, Sgonico (Trieste), Italy
phone: +39 040 2140406; fax: +39 040 2140365; e-mail: glaurenzano@inogs.it